# The Unimolecular Chemistry of Protonated Glycinamide and the Proton Affinity of Glycinamide—Mass Spectrometric Experiments and Theoretical Model

**Robin D. Kinser, Douglas P. Ridge, Georg Hvistendahl, Bård Rasmussen and Einar Uggerud***

**Abstract**: The potential energy hypersurface of protonated glycinamide ($GAH^+$) has been investigated experimentally and theoretically. The calculated G2(MP2) value for the proton affinity of glycinamide, $PA_{calcd} = 919\ kJ\,mol^{-1}$, is in good agreement with the measured value of $908 < PA_{exp} < 914\ kJ\,mol^{-1}$. The fact that the amide group is a better hydrogen-bond acceptor explains why glycinamide has a higher *PA* than glycine. Proton transfer experiments with glycinamide performed in a Fourier transform mass spectrometer and analysis of metastable $GAH^+$ ions in a four-sector mass spectrometer show that the lowest-energy unimolecular reactions are two distinct processes: 1) loss of CO, which has a substantial barrier for the reverse reaction, and 2) loss of CO plus $NH_3$, which has no barrier for the reverse reaction. Ab initio quantum chemical calculations give a reaction model that is consistent with the observed fragmentation pattern.

**Keywords**
ab initio calculations · glycinamide · mass spectrometry · protonations · quantum chemistry

## Introduction

The chemistry of protonated amino acids and peptides currently attracts much attention.[1, 2] Protonated peptides are routinely formed by a great variety of ionization methods including fast atom bombardement,[3] laser desorption,[4] electrospray,[5] chemical ionization[6] and plasma desorption.[7] Determination of the mass-to-charge ratio ($m/z$) of the $MH^+$ ions so formed gives important information on molecular weight. In addition a good deal of information about the structure of peptides can be gained from their mass spectral fragmentation patterns. Both the identity of the amino acids that constitute the peptide and their sequence can be determined in this way. Of special interest in this connection is the mechanism by which protonated peptides fragment. The complexity of these macromolecules poses a significant impediment to any detailed evaluation of the energetics or mechanisms of the reactions that generate the mass spectrum.

A peptide has a number of basic sites that can be protonated.[8] The fragmentation pattern is determined by a number of factors, namely, the kinetics and energetics of the initial proton transfer reaction and the subsequent (usually heterolytic) bond-breaking reactions. The availability (in both the thermodynamic and the kinetic sense) of the different basic sites as well as the lability towards homolytic cleavage of the protonated bonds are known to be important factors.[9, 10] Rearrangements within the protonated peptide prior to bond cleavage of molecular groups via electrostatically bonded ion/molecule complexes[11, 12, 13, 14] should be considered to be significant.

We have recently conducted a combined experimental and theoretical study of the unimolecular chemistry of protonated formamide.[15] Formamide is the simplest molecule that contains a peptide bond. The activation energies and mechanisms for the three unimolecular reactions observed, namely, loss of water, loss of ammonia, and loss of carbon monoxide, were determined. The reaction paths for loss of water and loss of ammonia start from the most stable O-protonated isomer, while the somewhat less stable N-protonated isomer is the precursor for CO loss.

As the next step in our project on fragmentation of protonated small-peptide prototype molecules, we have decided to look at a slightly more complex system, namely, protonated glycinamide ($GAH^+$). In addition to an amide bond this molecule contains a basic $-NH_2$ group. Our idea is to investigate the influence of the basic "side group" on the unimolecular chemistry, because many amino acids contain basic side groups which are known to influence all aspects of the chemistry of the peptide. The size of the molecular system permits the use of ab initio quantum chemical methods to model the reaction mechanisms. Applying different mass spectrometric methods in which the internal energy of the $GAH^+$ ion can be varied in a controlled manner allows us to check the predictions of the theoretical model.

[*] Prof. Dr. E. Uggerud, Prof. Dr. G. Hvistendahl, B. Rasmussen
Department of Chemistry, University of Oslo
P. O. Box 1033 Blindern, N-0315 Oslo (Norway)
e-mail: einar.uggerud@kjemi.uio.no
Prof. Dr. D. P. Ridge, Dr. R. D. Kinser
Department of Chemistry and Biochemistry
University of Delaware, Newark, DE 19716 (USA)

  0947-6539/96/0209-1143 $ 15.00+.25/0 

## Results and Discussion

**The proton affinity of glycinamide**: The proton affinity (*PA*) of glycinamide was determined by bracketing with a number of bases with known *PA*s by means of FTMS (Fourier transform mass spectrometry). Reactions (1–4) were observed. One com-

$$CH_3OH_2^+ + GA \longrightarrow GAH^+ + CH_3OH \quad (1)$$

$$C_2H_5NH_3^+ + GA \longrightarrow GAH^+ + C_2H_5NH_2 \quad (2)$$

$$GAH^+ + nC_4H_9NH_2 \longrightarrow nC_4H_9NH_3^+ + GA \quad (3)$$

$$GAH^+ + (CH_3)_2NH \longrightarrow (CH_3)_2NH_2^+ + GA \quad (4)$$

plication was encountered during these measurements: as the difference in proton affinity decreased, the formation of proton-bonded dimers of GA with itself and GA with the reference base was observed at long reaction times. A careful comparison of the ion abundancies as a function of pressure and reaction times was therefore undertaken. The results of this systematic analysis showed that the proton affinity of glycinamide lies midway between that of ethylamine ($PA = 908$ kJ mol$^{-1}$) and *n*-butylamine ($PA = 914$ kJ mol$^{-1}$).[16] Based on these measurements we estimate the proton affinity of glycinamide to be 911 kJ mol$^{-1}$. The proton affinity of glycinamide is significantly higher than that of glycine, which has been measured to lie in the range of 864–891 kJ mol$^{-1}$.[17, 18, 19, 20, 21]

To gain more insight into the factors that determine the value of the *PA*, we conducted a series of ab initio calculations on glycinamide (**1**) and on the three isomeric forms of protonated glycinamide **2**–**4**. The energy data are summarized in Table 1 and the structures are shown in Figure 1. It is evident that the most basic site of glycinamide is the nitrogen atom of the amino group. The resulting isomer **2** is 43 kJ mol$^{-1}$ more stable than the O-protonated form **3** (calculated at the MP2/6-31G(d,p) level), which in turn is 38 kJ mol$^{-1}$ more stable than the isomer **4** protonated at the amide nitrogen. Isomer **2** is stabilized by an intramolecular hydrogen bond to the oxygen atom, which is a better hydrogen-bond acceptor than the amide nitrogen, owing to its higher local proton affinity. We obtain an absolute proton affinity $PA_{calcd}$ of 953 kJ mol$^{-1}$ based on the most stable isomer

Table 1. Results from ab initio calculations.

| Molecule | *E*/Hartree [a] (HF/3-21G) | *E*/Hartree [b] (MP2/6-31G**) | *E*(z.p.v.) [c] /kJ mol$^{-1}$ |
|---|---|---|---|
| $NH_2CH_2CONH_2$ (**1**) | −261.52938 | −263.80606 | 232 |
| $NH_3^+CH_2CONH_2$ (**2**) | −261.91107 | −264.17954 | 268 |
| $NH_2CH_2COH^+NH_2$ (**3**) | −261.89895 | −264.16337 | 267 |
| $NH_2CH_2CONH_3^+$ (**4**) | −261.87620 | −264.14777 | 264 |
| $OC\cdots CH_2NH_2^+\cdots NH_3$ (**5**) | −261.88504 | −264.14982 | 244 |
| $CH_2NH_2^+\cdots NH_3$ (**6**) | −149.78803 | −151.12248 | 230 |
| $NH_2CH_2NH_3^+$ (**7**) | −149.79142 | −151.12468 | 245 |
| $CH_2NH_2^+$ (**8**) | −93.86284 | −94.69164 | 138 |
| $NH_3$ (**9**) | −55.87220 | −56.38322 | 88 |
| $NH_4^+$ (**10**) | −56.23386 | −56.73368 | 126 |
| CO (**11**) | −112.09330 | −113.02122 | 12 |
| $OC\cdots CH_2NH_2^+$ (**12**) | −205.96248 | −207.72158 | 154 |
| TS [**2** → **4**] | −261.87123 | −264.14183 | 255 |
| TS [**4** → **5**] | −261.83606 | −264.10751 | 251 |
| TS [**6** → **7**] | −149.76901 | −151.10393 | 232 |
| TS [**7** → **7**], $H^+$ transf. | −149.74772 | −151.08830 | 232 |

[a] Molecular potential energy obtained from geometry-optimized HF/3-21G structures. [b] Molecular potential energy obtained from geometry-optimized MP2(FC)/6-31G(d,p) structures. [c] Zero-point vibrational energies; vibrational frequencies were calculated for MP2/6-31G(d,p) optimized structures and scaled by a factor of 0.94.

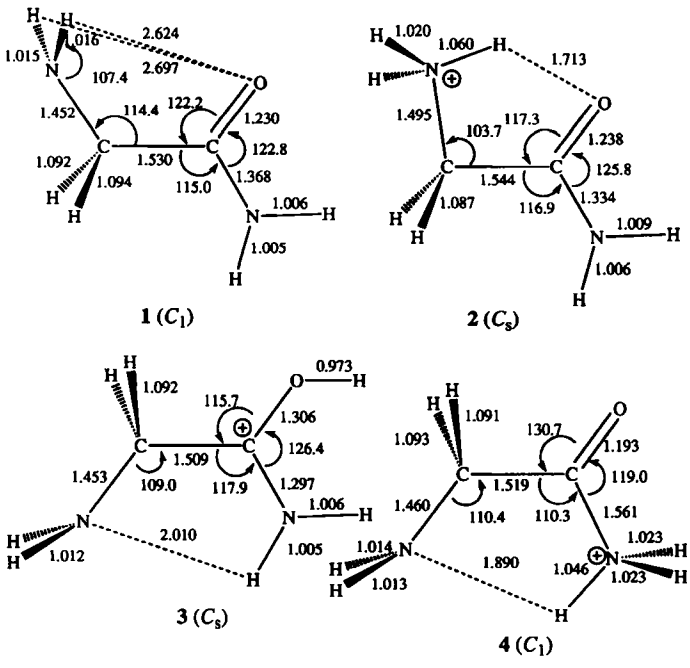


Fig. 1. Molecular structures (MP2/6-31G(d,p)) of glycinamide (**1**) and its three isomeric protonated forms **2**–**4**.

2. Absolute *PA*s obtained at this level of theory are known to be systematically overestimated.[22, 23] When we instead compare the calculated proton affinity of glycinamide with that of ammonia, we find the former to be 62 kJ mol$^{-1}$ higher. By comparison with the known experimental *PA* of ammonia, we estimate the theoretical proton affinity $PA_{calcd}$ of glycinamide to be 916 kJ mol$^{-1}$, which is in satisfactory agreement with our measured value $PA_{exp}$ of 911 kJ mol$^{-1}$.

It has been demonstrated that post-Hartree–Fock calculations with large basis sets generally give absolute theoretical *PA*s which are correct within 10–20 kJ mol$^{-1}$.[22, 23, 24] One method which has this potential is G2(MP2), and it was therefore used to calculate the energies of GA (**1**) and $GAH^+$ (**2**) (absolute energies are not tabulated), with the exception that vibrational frequencies were taken from MP2/6-31G(d,p) calculations. The absolute proton affinity obtained, $PA_{calcd} = 919$ kJ mol$^{-1}$, compares well with the experimental estimate.

The difference in proton affinity between glycinamide and glycine can be attributed to a stabilizing effect of the amide group (in glycinamide) relative to the carboxylic acid group (in glycine). Both protonated glycinamide (Fig. 2) and protonated glycine form intramolecular hydrogen bonds. The ab initio structure of **2** clearly shows the presence of a strong intramolecular hydrogen bond. The HF/3-21G hydrogen-bond length was found to be 1.750 Å. An equivalent calculation (HF/3-21G) of protonated glycine shows that in this case the corresponding hydrogen bond is weaker, as can be inferred from the significantly longer hydrogen bond of 1.922 Å.[25] The energy difference (HF/3-21G, uncorrected for zero-point vibrational energy) between glycine and its protonated form is 966 kJ mol$^{-1}$, while in glycinamide/protonated glycinamide the corresponding energy difference is 993 kJ mol$^{-1}$. It is well known that the oxygen atom of an amide is a better hydrogen-bond acceptor than the oxygen of a carboxylic acid group. This phenomenon is related to the partial double-bond character of the C–N bond and has been verified by crystallography[26] and by analysis of thermochemical data on intermolecular proton-bonded dimers in the gas phase.[27]



0947-6539/96/0209-1144 $ 15.00+.25/0 Chem. Eur. J. 1996, 2, No. 9

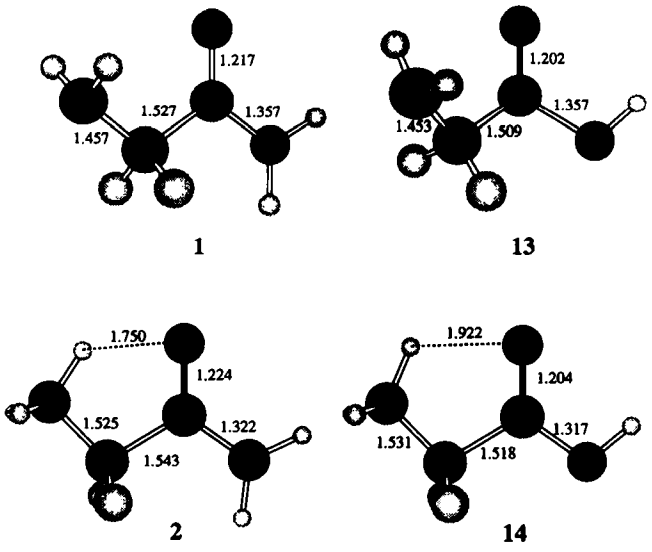


Fig. 2. HF/3-21G structures of glycinamide (**1**), protonated glycinamide (**2**), glycine (**13**), and protonated glycine (**14**). The last two structures were taken from ref. [25].

**Unimolecular fragmentation—experiment**: The proton transfer reactions reported so far only lead to protonated glycinamide or proton-bonded dimers of GA. When bases with sufficiently low proton affinities are used, unimolecular fragmentation reactions of excited $GAH^+$ ions are observed. In addition to reactions (1–4), reactions (5–7) were investigated.

$$N_2D^+ + GA \longrightarrow (GAD^+)^* + N_2 \longrightarrow \text{fragments} \quad (5)$$

$$CD_5^+ + GA \longrightarrow (GAD^+)^* + CD_4 \longrightarrow \text{fragments} \quad (6)$$

$$C_2D_5^+ + GA \longrightarrow (GAD^+)^* + C_2D_4 \longrightarrow \text{fragments} \quad (7)$$

Figure 3 shows the FT mass spectrum of glycinamide obtained after a 0.6 s reaction of $CD_5^+$ ($m/z = 22$) and glycinamide. An ion signal corresponding to $GAD^+$ is observed in the spectrum at $m/z = 76$. The peak at $m/z = 75$ corresponds to $GAH^+$ ions. The exothermic deuteron transfer reaction gives fragment ions corresponding to loss of carbon monoxide at $m/z = 48$ and to loss of carbon monoxide and either $NH_2D$ ($m/z = 30$) or $NH_3$ ($m/z = 31$). The ions formed by loss of carbon monoxide and ammonia correspond to the methylene immonium ion ($CH_2NH_2^+$) and its deuterated analogue ($CH_2NHD^+$).

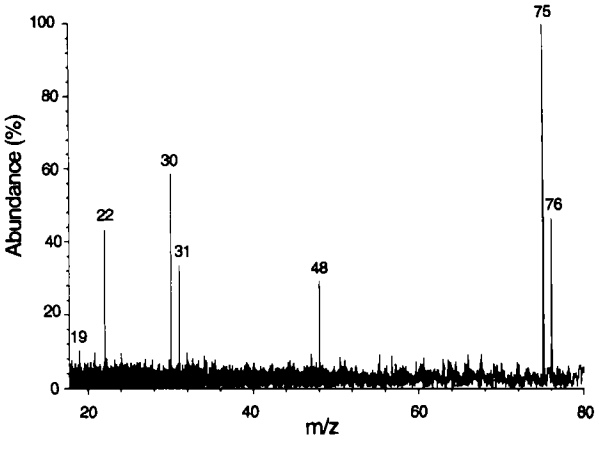


Fig. 3. FTMS spectrum obtained at $t_3 = 0.605$ s upon reaction between $CD_5^+$ and glycinamide.

It is evident from Figure 4 that $GAD^+$ ($m/z = 76$) behaves differently from $[GAD - CO - NH_2D]^+$ ($m/z = 30$) and $[GAD - CO]^+$ ($m/z = 48$). The fragment ions appear with a common pseudo first order rate constant ($k' = 1.1\ s^{-1}$), which corresponds to the rate that $CD_5^+$ disappears. This suggests that the fragments form from the product of deuteron transfer from $CD_5^+$ to GA in very fast unimolecular steps. The $GAD^+$ ion observed in the spectra is the result of subsequent reactions of the fragment ions with GA. The lines in Figure 4 represent the best fit of the data for this reaction sequence.

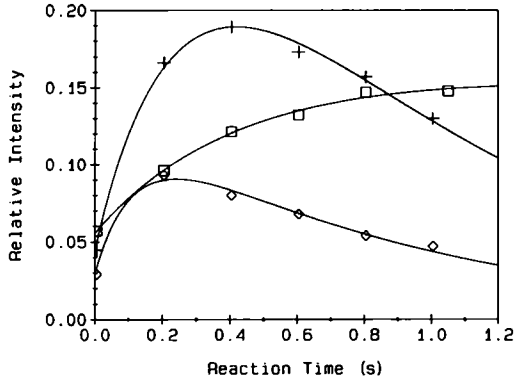


Fig. 4. Development of reaction products with time upon reaction between $CD_5^+$ and glycinamide in the FTMS cell: $GAD^+$ ($m/z = 76$, □), $[GAD - CO]^+$ ($m/z = 48$, ◇) and $[GAD - CO - NH_2D]^+$ ($m/z = 30$, +).

From Table 2 it can be seen that the effect of changing the proton (or deuteron) donor has a significant effect on the fragmentation pattern [Eqs. (8) and (9)]. It is evident that the

$$[NH_2CH_2CONH_2]D^+ (m/z\ 76) \longrightarrow [NH_2CH_2,NH_2D]^+ (m/z\ 48) + CO \quad (8)$$

$$[NH_2CH_2CONH_2]D^+ (m/z\ 76) \longrightarrow [CH_2NHD]^+ (m/z\ 31) + NH_3 + CO \quad (9a)$$

$$[NH_2CH_2CONH_2]D^+ (m/z\ 76) \longrightarrow [CH_2NH_2]^+ (m/z\ 30) + NH_2D + CO \quad (9b)$$

amount of $[CH_2NH_2]^+ + [CH_2NHD]^+$ relative to $[NH_2CH_2, NH_2D]^+$ increases with decreasing proton affinity of B, which favours the more endothermic process. The plot of Figure 4 shows that the $[CH_2NH_2]^+$ and $[CH_2NHD]^+$ fragments behave rather similarly. These observations tend to substantiate the hypothesis that the two fragmentation reactions have rather similar energetic requirements, but reaction (9) is favoured at higher energies. This could be explained by a mechanism in which the two reactions have approximately equal activation

Table 2. Reactivity of protonated glycinamide from the FTMS experiments.

| Reactant ion ($BH^+$) | $PA(GA) - PA(B)$/kJ mol$^{-1}$ | $A(9a+9b)/A(9a+9b+8)$ [a] |
|---|---|---|
| $N_2D^+$ | 416 | 0.96 |
| $CD_5^+$ | 360 | 0.84 |
| $C_2D_5^+$ | 231 | 0.39 |
| $CH_3OH_2^+$ | 150 | no fragments obs. |

[a] Relative abundance ions formed by loss of $CO + NH_3$ (and $NH_2D$) to all fragmentation products, obtained by fitting the kinetic model to the experimentally obtained temporal dependence of ion intensities. Reactions (8), (9a) and (9b) refer to the corresponding reactions in the text.

energies (reaction (9) has a slightly higher activation energy than reaction (8)), but reaction (9) occurs via a loose transition state and reaction (8) via a tight one.

Analysis of the data shows that $GAD^+$ produces the ions $CH_2NHD^+$ and $CH_2NH_2^+$ in a ratio of approximately 1:2. It is evident that partial deuterium atom scrambling does occur within the $[NH_2CH_2CONH_2]D^+$ ion, although the scrambling among the exchangable hydrogens is not complete, as is seen from the observed isotope distribution in the product. A complete hydrogen randomization would give a 2:3 ratio (four H and one D, of which three are lost when ammonia is expelled).

The daughter-ion spectrum of metastable $GAH^+$ ions recorded by the MIKE technique is reproduced in Figure 5. Also in this case, the ions $[NH_2CH_2,NH_3]^+$ ($m/z = 47$) and $[CH_2NH_2]^+$ ($m/z = 30$) are the only fragments observed, but in clearly different relative abundance from that found in the

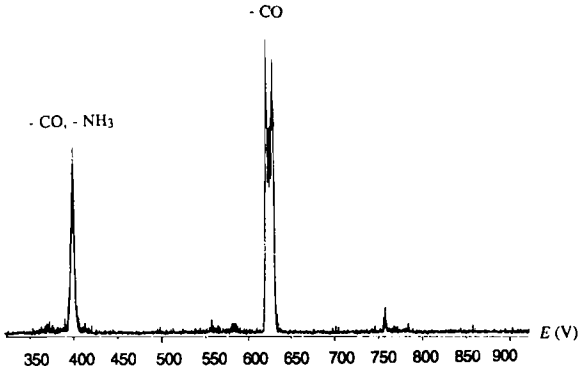


Fig. 5. Daughter-ion spectrum of metastable $GAH^+$ ions. The spectrum was obtained by the MIKE scan technique with the four-sector machine. The first two sectors were kept fixed only allowing transmittance of ions with $m/z = 75$ to the third field-free region. Unimolecular decomposition in the third field-free region was monitored by scanning the third sector (E). Full E voltage corresponds to 997.0 V.

FTMS experiments. In the latter all fragment ions produced in the unimolecular decomposition of $GAH^+$ ions are recorded. In the sector instrument, using the MIKE technique, the situation is different. Metastable ions are the ions that have survived the first few microseconds inside the ion source. Most of the high-energy $GAH^+$ ions already decompose in the ion source, so the metastable ions are selected from the low-energy part of the $GAH^+$ ion population. For this reason the low-energy processes dominate the fragmentation of metastable $GAH^+$ ions. The main peak ($m/z = 47$) in the daughter-ion spectrum is due to loss of CO. This finding supports a reaction model in which CO loss is the lower energy fragmentation pathway. However, the difference in critical energy is probably small since the processes are competing in the metastable region.

The translational energy release for CO loss [Eq. (8)] was determined from the width of the $m/z = 47$ peak in the MIKE spectrum to be $T_{0.5} = 32 \pm 2\ kJ\,mol^{-1}$. This rather high value indicates a reaction with a substantial barrier for the reverse reaction. On the other hand, the combined loss of the elements of CO and $NH_3$ [Eq. (9)], giving rise to the $m/z = 30$ peaks, only has $T_{0.5} = 4 \pm 1\ kJ\,mol^{-1}$; this indicates a process with zero or very low reverse barrier. It therefore appears that the processes leading to the $m/z = 47$ and $m/z = 30$ peaks are unrelated in the sense that the $[CH_2NH_2]^+$ ions are not formed in two steps, where reaction (8) is the first step and $NH_3$ loss from the resulting $[NH_2CH_2,NH_3]^+$ ion is the second. If they were related, the width of the $m/z = 30$ peak in the MIKE spectrum should reflect the high translational energy release accompanying the first step. It is also remarkable that there is no significant peak at $m/z = 58$, corresponding to $[H_2NCH_2{-}CO^+]$. This finding eliminates the possibility that ions with $m/z = 30$ might be formed by the sequential loss of $NH_3$ and CO, via an intermediate with a significant lifetime. We therefore conclude that $NH_3$ and CO are lost simultaneously, either in the form of the two separate molecules or as one single molecule (formamide is the only $CH_3NO$ isomer with a heat of formation lower than that of $CO + NH_3$).

Not shown here is the MIKE spectrum of protonated glycinamide labelled with $^{15}N$ in the amido group. A peak due to CO loss is observed at $m/z = 48$, while a peak at $m/z = 30$ comes from loss of CO and $^{15}NH_3$. A peak at $m/z = 31$ corresponding to loss of CO and $^{14}NH_3$ is absent; this indicates that the only source of ammonia loss in this case is from the amido group. As in the unlabelled case we determine $T_{0.5} = 32 \pm 2\ kJ\,mol^{-1}$ for the CO loss.

Ions of composition $[NH_2CH_2,{}^{15}NH_3]^+$ ($m/z = 48$) formed in the ion source as the result of CO loss from the protonated $^{15}N$-labelled parent molecule were also subject to MIKE analysis. The spectrum is reproduced in Figure 6. As expected a peak at $m/z = 30$ (corresponding to $CH_2NH_2^+$, due to $^{15}NH_3$ loss) is observed. In addition there is a smaller peak ($CH_2{}^{15}NH_2^+$, 15%) at $m/z = 31$, showing that loss of $^{14}NH_3$ also occurs. This observation indicates that partial equilibration of the two nitrogen atoms occurs within the $[NH_2CH_2,{}^{15}NH_3]^+$ ion prior to unimolecular decomposition.

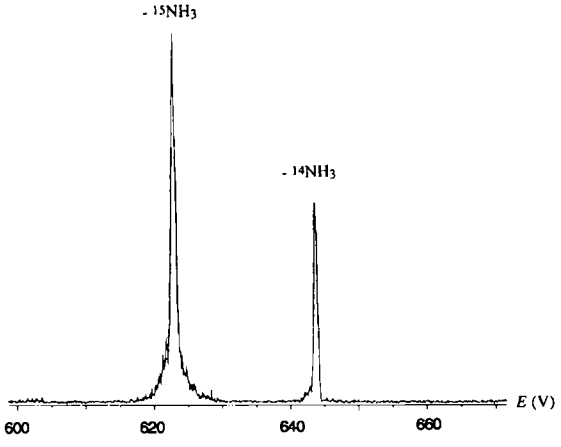


Fig. 6. Daughter-ion spectrum of metastable ions of nominal composition $[NH_2CH_2,{}^{15}NH_3]^+$. The spectrum was obtained by the MIKE scan technique with the four-sector machine. The first two sectors were kept fixed, only allowing transmittance of ions with $m/z = 48$ to the third field-free region. Unimolecular decomposition in the third field-free region was monitored by scanning the third sector (E). Full E voltage corresponds to 997.0 V.

The difference in appearance energies ($AE$) for the processes (10) and (11) was measured by variable low-energy collisions

$$[NH_2CH_2CONH_2]H^+ (m/z\ 75) \longrightarrow [NH_2CH_2,NH_3]^+ (m/z\ 47) + CO \quad (10)$$

$$[NH_2CH_2CONH_2]H^+ (m/z\ 75) \longrightarrow [CH_2NH_2]^+ (m/z\ 30) + CO + NH_3 \quad (11)$$

of $GAH^+$ ions with He by using the hybrid instrument.[28] In the absence of a reliable calibrant it was not possible to conduct measurements of absolute $AE$ with the required accuracy, but



0947-6539/96/0209-1146 $ 15.00+.25/0 Chem. Eur. J. 1996, 2, No. 9

the relative onsets for the $m/z = 47$ and $m/z = 30$ ions could be determined precisely. The measurements gave a difference between $AE(m/z\ 30)$ and $AE(m/z\ 47)$ of $19 \pm 5\ kJ\,mol^{-1}$; this shows that CO loss is the reaction with the lowest barrier.

**Unimolecular fragmentation—theoretical model**: The part of the potential energy hypersurface of $GAH^+$ which is relevant to the unimolecular chemistry was calculated at the MP2/6-31G(d,p) level of theory. The energy data were corrected for differences in zero-point vibrational energies and are reproduced in Table 1 and Figure 7.

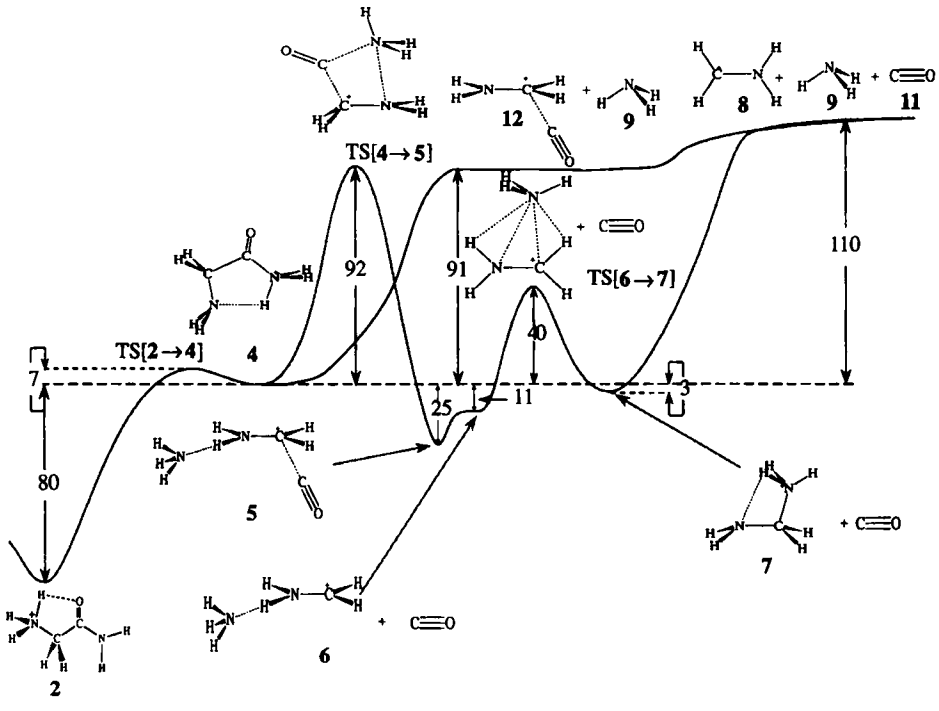


Fig. 7. Potential energy profile for unimolecular decomposition of $GAH^+$ obtained from the ab initio calculations (data in Table 1).

Starting from the most stable isomer of $GAH^+$ (the aminoprotonated form, **2**) loss of CO is shown to proceed in two steps. In the first step a proton is transferred to the amido site, and the isomer **4** is formed as an intermediate. Alternatively, isomer **4** is formed directly upon proton transfer. The key to the CO loss is the transition structure TS[**4** → **5**]. Its geometry is shown in Figure 8 and involves rearrangement of the amido $NH_3$ group. The energy of this transition structure is $172\ kJ\,mol^{-1}$ above that of **2**. In the rearrangement of **4** via TS[**4** → **5**], the isomer **5** is formed as a transient intermediate. CO is lost immediately from **5** owing to the almost vanishingly low C···C bond dissociation energy. The product ion has the structure $CH_2NH_2^+ \cdots NH_3$ (**6**), as determined by calculation

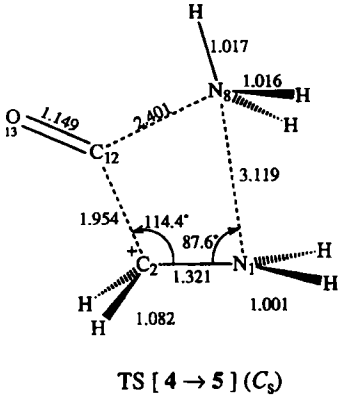


Fig. 8. MP2/6-31G(d,p) transition structure (TS[**4** → **5**]) for the ammonia rearrangement which precedes loss of CO from $GAH^+$.

of the intrinsic reaction-coordinate pathway. This rearrangement followed by fragmentation is seen to give rise to a substantial barrier for the reverse reaction ($116\ kJ\,mol^{-1}$). This is in agreement with the experimental observation that the reaction is accompanied by a significant translational energy release of $T_{0.5} = 32 \pm 2\ kJ\,mol^{-1}$ (which corresponds to approximately one third of the reverse barrier).

The fate of the $CH_2NH_2^+ \cdots NH_3$ ion (**6**) depends on the internal energy of the $GAH^+$ ions. If the internal energy is sufficiently high, ammonia may be lost in a second step, either directly or via the isomer **7**. Rearrangement of **6** to **7** only requires an activation energy of $51\ kJ\,mol^{-1}$. The products $CH_2NH_2^+ + CO + NH_3$ are only slightly above TS[**4** → **5**], so energy-rich $GAH^+$ ions will give rise to these products in agreement with the FTMS experiments. For ions with only a few $kJ\,mol^{-1}$ in addition to TS[**4** → **5**], the situation is different. During CO loss a sufficiently large proportion of the internal energy of the $GAH^+$ ion is given away to relative translation; these ions will therefore end up as unreactive $[NH_2CH_2,NH_3]^+$ ions. This is exactly what is observed in the MIKE experiments. Only energy-rich $GAH^+$ that loose CO in the ion source or in the FTMS cell will have sufficient energy to accomodate the complete sequence (12). For this reason an alternative and more

$$\begin{aligned}&[NH_2CH_2CONH_2]H^+ \longrightarrow\\ &[NH_2CH_2,NH_3]^+ + CO \longrightarrow\\ &\quad [NH_2CH_2]^+ + CO + NH_3\end{aligned} \qquad (12)$$

likely mechanism for loss of the elements of CO and $NH_3$ must exist for long-lived metastable $GAH^+$ ions, which decompose during flight through the analyser tube. Starting from isomer **4**, direct scission of the amide bond will give $[H_2NCH_2 \cdots CO]^+$ (**12**) + $NH_3$ (**9**). The absence of the intermediate **12** in the MIKE spectrum is in good agreement with the finding that this is a very weakly bonded complex. Loss of CO will therefore most likely occur directly upon $NH_3$ loss. Separate calculations show that the lengthening of the amide bond which precedes $NH_3$ loss leads to a simultaneous weakening of the bond between $[NH_2CH_2]^+$ and CO. The best description of the process is therefore that $NH_3$ and CO are lost simultanously, but through an asynchronous mechanism, where lengthening of the C···N bond precedes lengthening of the C···C bond. The reaction has no transition structure and is classified as a type I reaction, having a loose transition state. According to the MP2 calculations the potential energy of the products, $[NH_2CH_2]^+ + CO + NH_3$, is $18\ kJ\,mol^{-1}$ higher than TS[**4** → **5**]. This is in very good agreement with the experimental observations.

Direct loss of ammonia from isomer **2** to give $[CH_2CONH_2]^+$ (**15**) + $NH_3$ (**9**) can be ruled out, because this would require $380\ kJ\,mol^{-1}$, based on HF/3-21G calculations.

One possibility for the formation of $[NH_2CH_2]^+$ (**8**, $m/z = 30$) from $GAH^+$ could be by loss of formamide ($H(C{=}O)NH_2$, **16**). A transition structure TS[**3** → **8** + **16**] for the loss of for-

mamide was indeed located. Not unexpectedly, the barrier for this reaction is very high as it involves an unfavourable proton transfer to an electropositive centre (the carbonyl carbon of the formamide to be formed). The HF/3-21G barrier calculated is 350 kJ mol$^{-1}$ higher than both TS[**4** → **5**] and the products $[NH_2CH_2]^+ + CO + NH_3$. We can therefore rule out formamide loss as a possible mechanism.

Up to this point we have not explained the hydrogen isotope distribution in the product ions from GAD$^+$ (FTMS) in terms of the theoretical model. In all cases hydrogen isotope randomization is incomplete. Although hydrogen transfer within GAD$^+$ itself should proceed relatively easily according to the calculations, fragmention seems to be equally fast or faster. If it is assumed that all reactive GAD$^+$ ions are formed by incorporating the D$^+$ at the amido nitrogen, the proposed mechanism for CO loss would initially lead to formation of an ion of structure $[CH_2NH_2 \cdots NH_2D]^+$ (**6**). This ion may either decompose directly giving $CH_2NH_2^+$ as the only product, or may rearrange to $[H_2DNCH_2NH_2]^+$ (**7**). Decomposition of this ion would again give $CH_2NH_2^+$ as the only product. However, there is a route for internal proton (deuteron) transfer in this ion via the symmetrical TS[**7** → **7**] [Eq. (13)]. The TS is 83 kJ mol$^{-1}$ higher

$$^+H_3NCH_2NH_2 \longrightarrow NH_2CH_2NH_3^+ \qquad (13)$$

in potential energy than **7**. As already mentioned, complete randomization of the deuteron via this mechanism would imply a product ratio of 3:2 for $CH_2NH_2^+$ relative to $CH_2NHD^+$ formation, while a ratio of 2:1 is observed. The incomplete randomization may therefore partially be explained by the relative high barrier for the internal proton transfer. In addition, the loss of ammonia is a direct bond dissociation with a high frequency factor, while the internal hydrogen exchange proceeds via a tight transition state with a low frequency factor. Although the critical energy for the latter process is almost 30 kJ mol$^{-1}$ lower than that of the former, it thus appears that they occur on the same timescale.

Complementary evidence comes from the MIKE experiments with [$^{15}$N]glycinamide. The fragment ion formed in the ion source upon loss of CO would initially have the structure $[CH_2{}^{14}NH_2 \cdots {}^{15}NH_3]^+$ according to the proposed mechanism. If complete scrambling of the hydrogens takes place according to sequence (14), equal amounts of $^{14}NH_3$ and $^{15}NH_3$

$$[CH_2{}^{14}NH_2 \cdots {}^{15}NH_3]^+ \longrightarrow [{}^{15}NH_3CH_2{}^{14}NH_2]^+ = [{}^{15}NH_2CH_2{}^{14}NH_3]^+ \qquad (14)$$

would be lost. The experiments show that approximately 15% of the ammonia molecules are lost in the form of $^{14}NH_3$; this again indicates that there is incomplete hydrogen randomization.

## Experimental and Theoretical Methods

**FTMS study**: The proton transfer reactions were performed with a dual cell Fourier transform mass spectrometer (FTMS-2000, Extrel, Madison, Wisconsin, USA). The appropriate reactant gases were mixed in the analyser cell and proton-donor molecules (BH$^+$) were formed as the result of ion–molecule reactions initiated by a short electron beam pulse. By a careful choice of excitation pulse frequency widths and amplitudes, all ions, except the BH$^+$ ions, were ejected from the analyser and source cell. The proton donor molecules were transferred to the source cell, by opening the gate potential of the aperture plate between the two cells for a predetermined time. BH$^+$ and glycinamide (formed by evaporation of glycinamide·HCl from the heated direct-inlet probe at ca. 135 °C) were then allowed to react. The mass spectrum was recorded after a variable reaction time, $t_3$. In this way the product ion distribution could be obtained as a function of time. The pulse sequence used is shown in Figure 9. The same experimental procedure was used in the bracketing experiments. Note that when GAH$^+$ was used as the reactant ion it was formed by "self-CI" of glycinamide in the source cell, isolated and transferred to the analyser cell, where it was left to react with the reference base. All chemicals were of commercial grade and were used without further purification. The instrument was operated at sufficiently high resolution to identify all reactants and products by precise mass measurement.

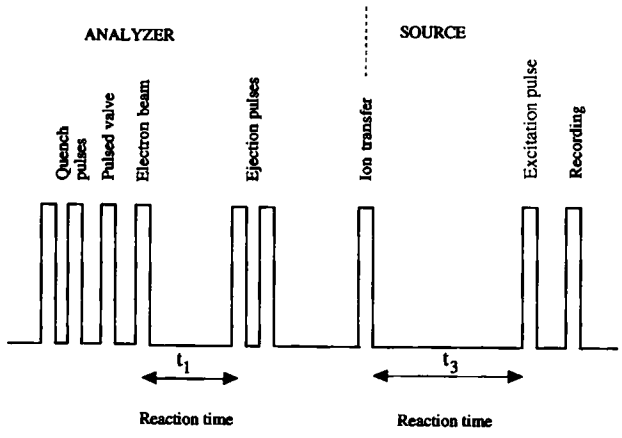


Fig. 9. Pulse sequence used in the FTMS experiments

**Study of metastable ions**: Protonated glycinamide ions (GAH$^+$, $m/z = 75$) and protonated $^{15}$N-labelled glycinamide ions ([$^{15}$N]GAH$^+$, $m/z = 76$) were produced by chemical ionization in the ion source of a hybrid EBEqQ sector mass spectrometer (VG Organic PROSPEC-Q, VG Analytical, Manchester, UK) or of a four-sector EBEB mass spectrometer (JEOL HX110/110). The reagent gas used was $CH_4$. The acceleration voltages were 8 kV (PROSPEC) and 10 kV (HX110/110). Scanning of the second E sector in either instrument (MIKE-scan) allowed analysis of the daughter ions produced by decomposition of metastable GAH$^+$ ions. All reactants were of commercial grade and were checked for purity by using both electron impact ionization (EI) and chemical ionization (CI). The amino $^{15}$N isotopomer of glycinamide was synthesized in steps according to literature procedures [29].

**Ab initio study**: The program systems Gaussian 92 [30] and Gaussian 94 were used for the calculations. The molecular geometries of all species relevant to the unimolecular chemistry of protonated glycinamide were first optimized using the 3-21G basis set [31] at the Hartree Fock (HF) level of theory [32]. Start geometries for the transition-structure optimizations were obtained by the linear synchronous transit method [33] or by crude interpolation of reactant and product geometries. A combination of the Newton algorithm and normal coordinate following algorithms were used for the all geometry optimizations. Starting from each of the optimized transition-structure geometries the intrinsic reaction coordinate [34] paths were calculated to ensure the correspondence between the transition structure and the reactant and the product structures. The optimized geometries were checked for the correct number of negative eigenvalues of the Hessian (the second derivative matrix). The HF/3-21G geometries were used as the starting geometries for the final stage of the optimizations. At this stage the wave functions were calculated using the Möller Plesset perturbation theory to the second order [35] with a 6-31G(d,p) basis set [36]. Analytical force constants were computed at this stage, and the vibrational frequencies were obtained. These vibrational frequencies were used for the final zero-point vibrational energy correction after scaling by a factor of 0.94 [37]. The optimized MP2/6-31G(d,p) geometries and energies together with the corresponding zero-point energies provide the final results. To obtain the highest-level theoretical estimate of the proton affinity G2(MP2) [24,38] calculations were in addition performed for glycinamide and the most stable isomer of protonated glycinamide.

**Acknowledgements**: E. U. wishes to thank the Norwegian Research Council (NRF) and VISTA for the grants which made this work possible. The calculations were made possible thanks to support through the NFR Programme for Supercomputing. The valuable assistance with the four-sector experiments from Dr. Tore Vulpius, Copenhagen, is highly appreciated.

Received: February 20, 1996 [F305]

[1] *Mass Spectrometry of Peptides* (Ed.: D. M. Desiderio), CRC Press, Boca Raton, **1991**.
[2] *Mass Spectrometry of Biological Materials* (Eds.: C. McEwen, B. Larsen), Marcel Dekker, New York, **1990**.
[3] M. Barber, R. S. Bordoli, R. D. Sedwick, A. N. Tyler, *J. Chem. Soc. Chem. Commun.* **1981**, 325.
[4] M. Karas, F. Hillenkamp, *Anal. Chem.* **1988**, *60*, 2299.
[5] S. F. Wong, C. K. Meng, J. B. Fenn, *J. Phys. Chem.* **1988**, *92*, 546.

[6] A. G. Harrison, *Chemical Ionization Mass Spectrometry*, CRC, Boca Raton, **1992**.
[7] G. P. Jonsson, A. B. Hedin, P. L. Håkansson, B. U. Sundquist, G. B. S. Save, P. F. Nielsen, P. Roepstorff, K.-E. Johansson, I. Kamensky, M. S. L. Lindberg, *Anal. Chem.* **1986**, *58*, 1084.
[8] R. W. Yeh, J. M. Grimley, M. M. Bursey, *Biol. Mass Spectrom.* **1991**, *20*, 443.
[9] H. Nakata, K.-I. Suzuki, N. Takeda, A. Tatematsu, *Org. Mass. Spectrom.* **1988**, *16*, 188.
[10] H. Nakata, K. Kadoguchi, H. Konishi, N. Takeda, A. Tatematsu, *Org. Mass Spectrom.* **1993**, *28*, 67.
[11] R. D. Bowen, J. Stapleton, D. H. Williams, *Tetrahedron Lett.* **1978**, , 2919.
[12] R. D. Bowen, D. H. Williams, H. Schwarz, C. Wesdemiotis, *J. Chem. Soc. Chem. Commun.* **1979**, 261.
[13] P. Longvialle, R. Botter, *J. Chem. Soc. Chem. Commun.* **1980**, 823.
[14] T. H. Morton, *J. Am. Chem. Soc.* **1983**, *102*, 1596.
[15] H. Y. Lin, D. P. Ridge, T. Vulpius, E. Uggerud, *J. Am. Chem. Soc.* **1994**, *116*, 2996.
[16] S. G. Lias, J. E. Bartmess, J. F. Liebman, J. H. Holmes, R. D. Levin, W. G. Mallard, *J. Phys. Chem. Ref. Data* **1988**, *17 (Supplement 1)*, 1.
[17] M. J. Locke, R. L. Hunter, R. T. McIver, *J. Am. Chem. Soc.* **1979**, *101*, 272.
[18] M. Meot-Ner, E. P. Hunter, F. Field, *J. Am. Chem. Soc.* **1979**, *101*, 686.
[19] G. S. Gorman, J. P. Speir, C. A. Turner, I. J. Amster, *J. Am. Chem. Soc.* **1992**, *114*, 3986.
[20] G. Bojesen, *J. Am. Chem. Soc.* **1987**, *109*, 5557.
[21] J. Wu, C. B. Lebrilla, *J. Am. Chem. Soc.* **1993**, *115*, 3270.
[22] E. Uggerud, *Mass Spectrom. Rev.* **1992**, *11*, 389.
[23] D. A. Dixon, S. G. Lias, in *Molecular Structure and Energetics, Vol. 2: Physical Measurements* (Eds.: J. L. Liebman, A. Greenberg) VCH, New York, **1987** pp. 269.
[24] B. J. Smith, L. Radom, *Chem. Phys. Lett.* **1994**, 231.
[25] S. Bouchonnet, Y. Hoppilliard, *Org. Mass Spectrom.* **1992**, *27*, 71.
[26] R. Taylor, O. Kennard, W. Versichel, *Acta Crystallogr.* **1984**, *B40*, 71.
[27] M. Meot-Ner, *J. Am. Chem. Soc.* **1984**, *106*, 1257.
[28] D. Ekeberg, S. I. Hagen, G. Hvistendahl, C. Schulze, E. Uggerud, J. Vedde, *Org. Mass Spectrom.* **1993**, *28*, 1547.
[29] B. Rasmussen, thesis, University of Oslo, **1995**.
[30] M. J. Frisch, G. W. Trucks, M. Head-Gordon, P. M. W. Gill, M. W. Wong, J. B. Foresman, B. G. Johnson, H. B. Schlegel, M. A. Robb, E. S. Replogle, R. Gomperts, J. L. Andres, K. Raghavachari, J. S. Binkley, C. Gonzalez, R. L. Martin, D. J. Fox, D. J. Defrees, J. Baker, J. J. P. Stewart, J. A. Pople, GAUSSIAN 92, Gaussian Inc., Pittsburgh, *PA*, **1992**.
[31] W. J. Hehre, R. Ditchfield, J. A. Pople, *J. Am. Chem. Soc.* **1972**, *56*, 2257.
[32] C. C. J. Roothan, *Rev. Mod. Phys.* **1951**, *23*, 69.
[33] T. A. Halgren, W. M. Lipscomb, *Chem. Phys. Lett.* **1977**, *49*, 225.
[34] C. Gonzales, H. B. Schlegel, *J. Phys. Chem.* **1989**, *90*, 2154.
[35] C. Möller, M. S. Plesset, *Phys. Rev.* **1934**, *46*, 618.
[36] M. J. Frisch, J. A. Pople, J. S. Binkley, *J. Chem. Phys.* **1984**, *80*, 3265.
[37] J. A. Pople, A. P. Scott, M. W. Wong, L. Radom, *Isr. J. Chem.* **1993**, *33*, 345.
[38] L. A. Curtiss, K. Raghavachari, J. A. Pople, *J. Chem. Phys.* **1993**, *98*, 1293.